# Laminar pipe flow with time-dependent viscosity

Alan E. Vardy and James M. B. Brown


## ABSTRACT

A general solution is obtained for laminar flow in axisymmetric pipes, allowing for prescribed time-dependent viscosity and time-dependent pressure gradients. In both cases, the only restriction on the prescribed time dependence is that it must vary continuously; it is not necessary for *rates of change* to be continuous. The general solution is obtained using the Finite Hankel Transform method. This makes it possible to allow explicitly for time-dependent viscosity, but it does not permit the spatial dependence of viscosity. This contrasts with Laplace transforms, which allow spatial, but not general, temporal variations. The general solution is used to study a selection of particular flows chosen to illustrate distinct forms of physical behaviour and to demonstrate the ease with which solutions are obtained. The methodology is also applied to the simple case of constant (Newtonian) viscosity. In this case, it yields the same solutions as previously published methods, but it does so in a much simpler manner.


**Key words** | Finite Hankel Transform, laminar flow, pipe flow, pulsating viscosity, starting flow, time dependence

**Alan E. Vardy** (corresponding author)
**James M. B. Brown**
Civil Engineering Division,
University of Dundee,
Dundee DD1 4HN,
UK
E-mail: *a.e.vardy@dundee.ac.uk*

## NOMENCLATURE

| | |
|---|---|
| $a$ | pipe radius |
| $B$ | non-dimensional rate of increase of viscosity defined in Equation (26) |
| $f$ | general function |
| $\bar{f}$ | Hankel Transform of function $f$ |
| $g_i$ | dimensional zero of $J_0\{ag\}$ |
| i | $\sqrt{(-1)}$ |
| $J_0\{\}$, $J_1\{\}$ | Bessel functions of first kind, and first and second order |
| $k_i$ | parameter defined in Equation (37) |
| $n\{\}$ | viscosity function defined in Equation (1) |
| $n_1\{\}$ | variable part of the viscosity function |
| $p$ | pressure |
| $P\{\}$ | pressure gradient function defined in Equation (2) |
| $P_0$,$P_1$ | coefficients in definition of linear $P\{t\}$ |
| $P_A$ | coefficient in definition of oscillating $P\{t\}$ |
| $r$ | radial coordinate |
| $t$ | time |
| $T$ | non-dimensional time defined in Equation (22) |
| $u$ | axial velocity |
| $\bar{u}$ | Hankel transform of the axial velocity |
| $U$ | cross-sectional mean axial velocity |
| $z$ | axial coordinate |

### Greek characters

| | |
|---|---|
| $\beta_1$ | coefficient in definition of linear $n\{t\}$ |
| $\beta_0$, $\beta_A$ | coefficients in definition of pulsating $n\{t\}$ |
| $\lambda_i$ | non-dimensional zero of $J_0\{\lambda\} = 0$ |
| $\nu$ | fluid kinematic viscosity |
| $\nu_1$ | variable part of the fluid kinematic viscosity |
| $\psi$, $\theta$ | dummy time variables |
| $\omega$ | angular frequency |
| $\omega_p$ | forcing angular frequency, pressure gradient |
| $\omega_\nu$ | forcing angular frequency, viscosity |
| $\rho$ | fluid density |
| $\tau$ | shear stress |

doi: 10.2166/hydro.2010.073

### Subscripts

| | |
|---|---|
| 0 | initial or constant |
| $i$ | member of a set |
| $w$ | wall |

## INTRODUCTION

In analyses of flows of fluids such as water and air, it is usually assumed that the fluid viscosity is constant. In general, however, there are situations in which it is necessary to allow for variations of viscosity during flow processes. For example, the viscosity can vary significantly with temperature and so may be influenced by compression, conduction and viscous heating. Examples of the consequences of temperature dependence can be found in geophysical processes, e.g. magma flows (e.g. Costa & Macedonio 2003; Costa *et al.* 2007) and in conduits generally (Adegbie & Alao 2006). In principle, viscosity can also vary with pressure. However, this is significant only at extremes of pressure far beyond flows of most common engineering interest. Consequences of pressure dependence in pipe flows have been investigated by, for example, Vasudevaiah & Rajagopal (2005), Massoudi & Phuoc (2006) and Suslova & Tran (2008). Pressure dependence in power station combustion processes can result in pulsating fluid viscosities, as studied by Ng (2004). Viscosity can also depend on changes in fluid composition and/or microstructure during a flow, as occurs in many rheological processes, e.g. Schowalter (1977), Butler & O'Donnell (1999), Phan-Thien (2002) and Maingonnat *et al.* (2005) (see also a review article by Barnes (1997)).

When the interpretation of "viscosity" is extended to include "turbulent eddy viscosity" almost all *unsteady* flows exhibit time-dependent viscosity. This raises major problems for analysts, whether using analytical or numerical methods of solution. The authors are not aware of any general *analytical* solutions that allow simultaneously for spatial and temporal viscosity dependence and most *numerical* solutions utilise turbulence closure models that have been calibrated using measurements of steady flows. This is a cause for concern because strong spatial and temporal variations can occur simultaneously, even in simple unsteady flows, e.g. uniformly accelerating flows (He *et al.* 2008). In any case, the nature of numerical solutions is such that each is restricted to its own particular set of boundary conditions. As a consequence, it is less easy to infer generic trends from numerical solutions than from analytical ones.

In the following analysis, attention is focused on axisymmetric flows rather than on planar 2D flows even though this increases the complexity of the analysis. The principal advantage of this is that more physical applications are found for pipes and ducts than for flows between parallel surfaces. First, the governing equations for incompressible laminar flow in a pipe are established, allowing for time-dependent viscosity and pressure gradient. Alternative methods of solution are reviewed briefly and an integral transform method is used to obtain a general solution for the velocity as a function of time, radial position and pressure gradient. The solution contains integrals over time of user-prescribed functions describing variations of viscosity and pressure gradient, respectively. Physically meaningful functions will be continuous and well defined and so the required integrals can always be evaluated.

This paper continues with illustrations of the application of the general solution for two forms of time-dependent viscosity (plus constant viscosity) and for three forms of varying pressure gradient. Key features of the resulting behaviour are discussed and conclusions are drawn.

## UNSTEADY, LAMINAR PIPE FLOW – GOVERNING EQUATIONS

Consider unidirectional, laminar flow in a smooth-walled tube of circular cross section with inner radius $a$. The flow is assumed incompressible and the axial velocity $u$ is a function of radial position $r$ and time $t$, but is uniform axially. The fluid has density $\rho$ and molecular kinematic viscosity $\nu_0$. The effective kinematic viscosity $\nu\{t\}$ is uniform in space, but may vary in time in a prescribed manner. The prescribed function $\nu_1\{t\}$ is conveniently scaled as

$$n\{t\} \equiv \frac{\nu\{t\}}{\nu_0} = \frac{\nu_0 + \nu_1\{t\}}{\nu_0} = 1 + n_1\{t\} \tag{1}$$

where $n\{t\}$ is a viscosity function and its variable part, $n_1\{t\}$, is assumed to be continuous although its derivatives need not be continuous. Note that, throughout this work, braces "{ }" are used to distinguish functional dependence from algebraic groupings using parentheses "( )" and brackets "[ ]". This

assists in the interpretation of various equations (see Equation (12), for instance).

For fully developed incompressible laminar flow in a pipe, the Navier–Stokes equations of motion show that, in the absence of significant body forces, the pressure is uniform over the pipe cross section and is a linear function of the axial coordinate $z$. Consequently the pressure gradient is uniform along the pipe. A pressure gradient function, which, in general, may be time-dependent, is conveniently defined as

$$P\{t\} - \frac{1}{\rho}\frac{\partial p}{\partial z}\{t\} \tag{2}$$

After incorporating Equations (1) and (2), the axisymmetric Navier–Stokes equations reduce to

$$\frac{\partial u}{\partial t} = P\{t\} + \nu_0 n\{t\}\frac{1}{r}\frac{\partial}{\partial r}\left(r\frac{\partial u}{\partial r}\right) \tag{3}$$

where $u = u\{r,t\}$ is the velocity in the axial direction $z$. A no-slip condition is applied at the pipe wall ($r = a$), a symmetry condition is used at the pipe axis ($r = 0$) and the initial velocity distribution is $u_0\{r\}$. That is

$$u\{a,t\} = 0; \qquad \frac{\partial u}{\partial r}\{0,t\} = 0; \qquad u\{r,0\} = u_0\{r\}. \tag{4}$$

The determination of a general solution for unsteady flow in a pipe requires the solution of Equation (3) subject to the conditions of Equation (4).

## Finite Hankel transforms

Equation (3) is a linear, non-homogeneous, second-order partial differential equation (PDE) in the axial velocity, but it has a time-dependent coefficient $n\{t\}$. The usual options for the solution of a linear PDE are by the separation of variables or by the use of integral transforms. In the present case, solution by separation of variables would be possible in principle since the non-constant coefficient depends only on time. Usually, however, engineers prefer an integral transform approach and, in the case of time-dependent PDEs, they most often use Laplace transforms in time. In this instance, this would be difficult, if not impossible, because of the term containing the product of the viscosity function $n\{t\}$ and the unknown velocity, both of which are time-dependent. Although Laplace transforms are possible for special time-dependent cases such as $t^n f\{t\}$, the authors are unaware of transforms for cases with more general time-dependent coefficients or for cases where the variable is a function of both space and time (i.e. $f\{r,t\}$).

Herein, an alternative integral transform approach, namely Finite Hankel Transforms (FHT) *in space*, e.g. Sneddon (1951, 1972) and Debnath & Bhatta (2007), is used to avoid the above difficulty. The FHT imposes no constraint on the viscosity function $n\{t\}$ and has the hugely valuable practical property that the inverse transform process is straightforward (see Equation (7)). The FHT of a function $f\{r,t\}$ is defined as

$$\bar{f}\{g_i,t\} \equiv \int_0^a f\{r,t\} r \mathrm{J}_0\{g_i\, r\}\mathrm{d}r, \quad i = 1,2,3,\ldots \tag{5}$$

where $g_i$ denotes the positive roots of the equation

$$J_0\{ag\} = 0 \tag{6}$$

and $\mathrm{J}_0$ is the Bessel function of the first kind and zero order. The product $ag$ is non-dimensional and is often denoted by the symbol $\lambda$. This practice is not followed herein (except in specific cases where it assists in clarity) because the formulation using a dimensional approach is easier to interpret physically. It is noteworthy that the dependence of $f$ on time $t$ does not influence the evaluation of the integral in Equation (5).

The inverse transform (IFHT) is defined as

$$u\{r,t\} \equiv \frac{2}{a^2}\sum_{i=1}^{\infty}\frac{\bar{u}\{g_i,t\}\mathrm{J}_0\{r g_i\}}{\mathrm{J}_1\{a g_i\}^2} \tag{7}$$

where $\mathrm{J}_1$ is a Bessel function of the first kind and first order. Note that this is much simpler than the Bromwich integral required to invert Laplace transforms.

Finite Hankel transforms have been used by other authors for studies of particular time-dependent flows. However, the authors are not aware of any other *general* solution such as that developed in the following section. Chambré *et al.* (1978) used the FHT approach to model a constant and uniform viscosity fluid under the action of (i) a suddenly imposed pressure gradient and (ii) a ramp pressure gradient. Fetecau (2004) used the Fourier–Bessel series (which is the basis for FHTs) to solve a particular boundary value problem for the flow of a non-Newtonian fluid (second-grade fluid) in a pipe. However, the fluid concerned did not have explicit

time dependence of the viscosity. Fetecau & Fetecau (2005) applied Fourier sine transforms to flows in plane geometry such as between parallel planes. Subsequently, Erdogan & Imrak (2007*a*) compared the use of the Laplace transform and the Fourier (in effect Hankel) transform for pipe flows, again with no explicit time dependence of the material properties. They focused on an evaluation of the relative mathematical convenience of the two methods. The same authors (Erdogan & Imrak 2009) also compared the use of Laplace transforms and Fourier sine transforms in the context of a plane geometrical flow. In all of these papers, the viscosity does not vary in time so both Laplace and Hankel transform methods are applicable in principle.

## GENERAL SOLUTION

The FHT of the equation of motion (3) can be written as

$$\frac{d\overline{u}\{g_i,t\}}{dt} = P\{t\}\int_0^a rJ_0\{g_i r\}\mathrm{d}r + \nu_0 n\{t\}\int_0^a \frac{1}{r}\frac{\partial}{\partial r}\left(r\frac{\partial u}{\partial r}\right)rJ_0\{g_i r\}\mathrm{d}r. \tag{8}$$

This result has the important advantage that the viscosity function $n\{t\}$ does not appear in the required integrations. A second valuable advantage is that the equation to be solved is reduced to first order.

In this section, the integrals in Equation (8) are solved and a general solution of the boundary value problem constituted by Equations (3) and (4) is derived. As a preliminary step, the integrals on the right-hand side of the equation are evaluated. Using, for instance, Abramowitz & Stegun (1972) or the Table of finite Hankel transforms in Sneddon (1951), the first of these integrals yields

$$\int_0^a rJ_0\{g_i r\}\mathrm{d}r = \frac{a}{g_i}J_1\{ag_i\}. \tag{9}$$

If required, the second integral on the RHS of Equation (8) could be evaluated by integration by parts and could be simplified using the two boundary conditions in Equation (4). However, this is not necessary because the evaluation is a standard operational result – see the tables of FHTs in Sneddon (1951) or Debnath & Bhatta (2007), for instance. The result may be expressed as

$$\int_0^a \frac{1}{r}\frac{\partial}{\partial r}\left(r\frac{\partial u}{\partial r}\right)rJ_0\{g_i r\}\mathrm{d}r = ag_i u\{a,t\}J_1\{ag_i\} - g_i^2\overline{u}\{g_i,t\}. \tag{10}$$

Using the no-slip boundary condition from Equation (4) in Equation (10) and substituting Equations (9) and (10) into Equation (8) leads to

$$\frac{d\overline{u}\{g_i,t\}}{dt} + \nu_0 n\{t\}g_i^2\overline{u}\{g_i,t\} = \frac{aP\{t\}}{g_i}J_1\{ag_i\} \tag{11}$$

which is a first-order non-homogeneous linear ordinary differential equation (ODE) (with a variable coefficient) for the FHT of the axial velocity. The solution is found by standard methods, e.g. Boyce & DiPrima (1969), to be

$$\overline{u}\{g_i,t\} = \exp\left\{-g_i^2\nu_0\int_0^t n\{\theta\}\mathrm{d}\theta\right\}\left(\frac{aJ_1\{ag_i\}}{g_i}\int_0^t \exp\left\{g_i^2\nu_0\int_0^\theta n\{\psi\}\mathrm{d}\psi\right\}P\{\theta\}\mathrm{d}\theta + \overline{u}_0\right) \tag{12}$$

where $\overline{u}_0$ is the initial condition. On physical grounds, the prescribed viscosity and pressure gradient functions will be continuous. Once they have been prescribed, the integrals in Equation (12) become quadratures. That is, they are equivalent to finding areas under continuous curves. Hence the integrals can always be evaluated numerically to any desired degree of accuracy and, for some prescribed forms of $n\{t\}$, $P\{t\}$ and the initial condition, explicit analytic expressions can be found.

The actual velocity then follows from the inverse FHT defined in Equation (7), viz

$$u\{r,t\} = \frac{2}{a^2}\sum_{i=1}^{\infty}\frac{\overline{u}\{g_i,t\}J_0\{rg_i\}}{J_1\{ag_i\}^2}. \tag{13}$$

Since the transformed velocity does not depend on position in the cross section, expressions for physically important kinematic parameters can be obtained term by term from Equation (13). For example, the mean velocity is obtained from the integral of $rJ_0\{rg_i\}$ over the pipe cross section, giving

$$U\{t\} = \frac{4}{a^3}\sum_{i=1}^{\infty}\frac{\overline{u}\{g_i,t\}}{g_i J_1\{ag_i\}} \tag{14}$$

and the velocity gradient at the wall, obtained from the derivative of $J_0\{rg_i\}$ with respect to $r$ evaluated at the pipe

wall, is

$$\frac{\partial u}{\partial r}\{a,t\} = -\frac{2}{a^2}\sum_{i=1}^{\infty}\frac{g_i\overline{u}\{g_i,t\}}{\mathrm{J}_1\{ag_i\}} \tag{15}$$

The acceleration of the mean flow is the time derivative of Equation (14), i.e.

$$\frac{\mathrm{d}U}{\mathrm{d}t} = \frac{4}{a^3}\sum_{i=1}^{\infty}\frac{\mathrm{d}\overline{u}\{t,g_i\}/\mathrm{d}t}{g_i\mathrm{J}_1\{ag_i\}}. \tag{16}$$

The wall shear stress is an important parameter in many fluid flows. In principle, it can be obtained from the wall velocity gradient Equation (15) and the viscosity function Equation (1) as

$$\tau_w\{t\} = \rho_0 v_0 n\{t\}\frac{\partial u}{\partial r}\{a,t\}. \tag{17}$$

Alternatively, it can be obtained directly from the momentum equation – see, for example, Achard & Lespinard (1981) – as

$$\tau_w\{t\} = \frac{\rho a}{2}\left(P\{t\} - \frac{\mathrm{d}U\{t\}}{\mathrm{d}t}\right). \tag{18}$$

In practice, the second of these methods is found to be more convenient computationally than the former.

### Numerical evaluation

Although the solution is analytical, its practical use in symbolic algebra packages or in advanced spreadsheets involves the evaluation of series of Bessel functions and exponential terms, etc. In principle, this introduces the possibility of convergence problems at very small and very large times. This is one reason for preferring Equation (18) to Equation (17). Nevertheless, the only cases for which the authors have encountered convergence problems are the evaluation of velocities (i) at very small times when a flow accelerates from rest and (ii) at very large times when a flow approaches a constant asymptotic condition. In the first of these cases, the difficulty is easily overcome by noting that the shear stress is necessarily negligible at very small times. In the second, it is overcome by noting that differences between the shear stress and its quasi-steady counterpart must be negligible.

In all cases, i.e. not only the two special cases cited in the preceding paragraph, it is necessary to ensure that the integrals are evaluated to sufficient accuracy. There are several methods of assessing convergence in principle, but the authors prefer the simple approach of evaluating a predetermined number of terms and confirming retrospectively that the number is much larger than is strictly necessary. This is nominally wasteful, but it has negligible impact on the performance of symbolic algebra software, so it is very convenient. Typically, the summation converges rapidly at large times, but more slowly at small times. For the examples presented herein, the largest number of terms required to achieve convergence to 0.1% at the smallest time considered is 13.

## STEP APPLICATION OF PRESSURE GRADIENT

The remainder of this paper presents particular examples of the application of the general solution and highlights the associated physical behaviour. In principle, the prescribed time dependence of the viscosity and of the forcing pressure gradient may have any continuous form. In practice, however, illustrations based on highly complex variations would be pointless because the interpretation of the resulting flows would be impracticable. Accordingly, the most complex case considered herein has periodically varying viscosity and periodically varying pressure gradient. Before considering that case, however, simpler cases are investigated, using the constant, step and linear variations shown in Figure 1. In this section, attention focuses on the particular case of a suddenly applied pressure gradient and, in the next section, a linearly increasing pressure gradient is considered. Solutions are investigated for both constant and time-dependent viscosity.

Suppose that a constant pressure gradient is suddenly imposed on a fluid that is initially at rest. The use of the analysis with a non-zero initial velocity distribution is straightforward, but for simplicity only the simpler condition, commonly referred to as the starting flow problem, is presented. The particular case of laminar pipe flow of a Newtonian fluid with *constant* viscosity was solved by Szymanski (1932) and solutions have been found for certain non-Newtonian fluids, e.g. Hayat *et al.* (2006) and Erdogan & Imrak (2007*b*).

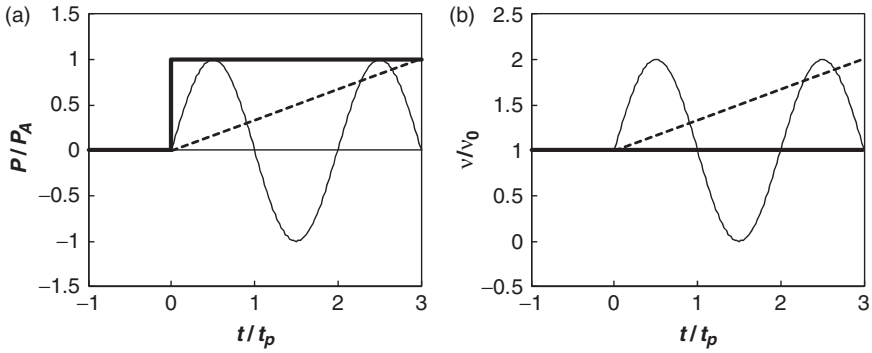


**Figure 1** | Prescribed pressure gradient and viscosity histories: (a) pressure gradient histories scaled by maximum value and (b) viscosity histories scaled by initial value.

Denoting the constant pressure gradient by $P_0$, Equation (12) reduces to

$$\overline{u}\{g_i,t\} = \frac{P_0 a \mathrm{J}_1\{ag_i\}}{g_i} \exp\left\{-g_i^2 v_0 \int_0^t n\{\theta\}\mathrm{d}\theta\right\} \left(\int_0^t \exp\left\{g_i^2 v_0 \int_0^\theta n\{\psi\}\mathrm{d}\psi\right\}\mathrm{d}\theta\right). \quad (19)$$

This is now solved firstly for constant viscosity (equivalent to the Szymanski case) and then for a linearly increasing viscosity.

## Constant viscosity

When the viscosity is constant, the functions $n\{\theta\}$ and $n\{\psi\}$ in Equation (19) are unit valued and the FHT of the velocity reduces to

$$\overline{u}\{g_i,t\} = \frac{P_0 a \mathrm{J}_1\{ag_i\}}{v_0 {g_i}^3}(1-\exp\{-g_i^2 v_0 t\}). \quad (20)$$

Using Equation (7), the velocity is given by the series

$$u\{r,t\} = \frac{2P_0}{a v_0}\sum_{i=1}^{\infty}\frac{(1-\exp\{-g_i^2 v_0 t\})\mathrm{J}_0\{rg_i\}}{g_i^3 \mathrm{J}_1\{ag_i\}} = \frac{2P_0 a^2}{v_0}\sum_{i=1}^{\infty}\frac{(1-\exp\{-\lambda_i^2 T\})\mathrm{J}_0\{\lambda_i r/a\}}{\lambda_i^3 \mathrm{J}_1\{\lambda_i\}} \quad (21)$$

where $T$ is a non-dimensional time defined as

$$T \equiv \frac{v_0 t}{a^2} \quad (22)$$

and $\lambda_i = ag_i$ is a zero of the equation

$$\mathrm{J}_0\{\lambda\} = 0. \quad (23)$$

Note that the zeros of Equation (23) are dimensionless whereas the zeros of Equation (6), i.e. $g_i$, are dimensional quantities, namely $\lambda_i$ scaled by the pipe radius $a$. Equation (21) is consistent with the well-established solution obtained by Szymanski (1932) and presented in a more modern format by Achard & Lespinard (1981). However, the above derivation using FHTs is more straightforward and more compact than the methods used previously.

Following the imposition of the step change in pressure gradient at $t$=0, the velocity evolves to a steady state condition satisfying

$$u\{r,t\}_{t\to\infty} = \frac{2P_0}{a v_0}\sum_{i=1}^{\infty}\frac{\mathrm{J}_0\{rg_i\}}{g_i^3 \mathrm{J}_1\{ag_i\}} = \frac{2P_0 a^2}{v_0}\sum_{i=1}^{\infty}\frac{\mathrm{J}_0\{\lambda_i r/a\}}{\lambda_i^3 \mathrm{J}_1\{\lambda_i\}} \quad (24)$$

which is the Fourier–Bessel expansion (e.g. Sneddon 1951) of the Poiseuille velocity distribution for steady laminar flow in a pipe of circular cross-section. The notation $\lambda_i = ag_i$ is used in the final term of Equation (24) for ease of comparison with the stated reference.

Each term in the series in Equation (21) decays quite rapidly with increasing time. Consider, for instance, the time required for the velocity to increase to 95% of its asymptotic value. This will certainly occur when the exponential terms $\exp\{-\lambda_i^2 T\}$ in the second form of Equation (21) have reduced to 0.05. For the first term in the summation (i.e. for $\lambda_1$), the required non-dimensional time is approximately $T$=0.518. All subsequent terms correspond to larger values of $\lambda$ and hence decay more rapidly. For example, the corresponding decay times for $\lambda_2$ and $\lambda_3$ are approximately 0.098 and 0.040. Thus the non-dimensional time for the change to be 95% complete will be of the order of 0.5. Accordingly, $T$=0.5

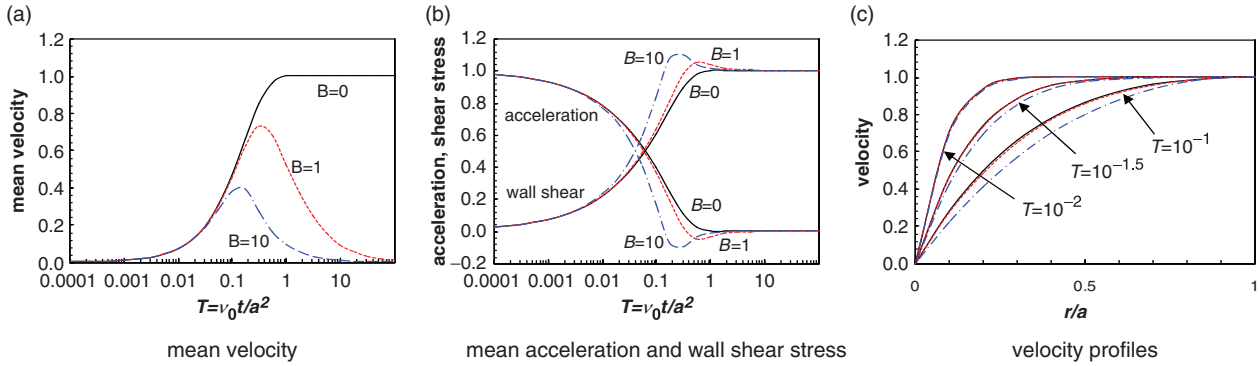


**Figure 2** | Starting flows resulting from a step pressure gradient [$B$=0 (continuous lines), $B$=1 (dotted lines), $B$=10 (dashed–dotted lines)]: (a) mean velocity, (b) mean acceleration and wall shear stress, and (c) velocity profiles.

may be used as a representative relaxation time for the system.

Predicted evolutions of the mean velocity, mean acceleration and velocity profile are shown as the case labelled $B$=0 in Figure 2. They are discussed in the following section as limiting cases of behaviour with time-varying viscosity.

## Linearly increasing viscosity

As a second illustration of the use of Equation (19), consider a flow in which the viscosity increases in time – as a result of continuous cooling, say. For a linear increase, the viscosity function satisfies

$$n\{t\} \equiv 1 + \beta_1 t = 1 + BT \tag{25}$$

where $\beta_1$ is a positive constant with dimension of $s^{-1}$, $T$ is non-dimensional time as in Equation (22) and $B$ is a dimensionless coefficient defined as

$$B \equiv \frac{a^2\beta_1}{\nu_0}. \tag{26}$$

The FHT of the velocity is found by substituting Equation (25) into Equation (19). Due to the complicated nature of some terms, it is convenient in this case to express the result using the non-dimensional time $T$ of Equation (22) and the non-dimensional Bessel function zeros $\lambda_i = ag_i$ leading to

$$\overline{u}\{\lambda_i, t\} = \frac{P_0 a^4 \mathrm{J}_1\{\lambda_i\} \exp\{-\lambda_i^2(1+BT)^2/2B\}}{\mathrm{i}\nu_0\lambda_i^2\sqrt{2/\pi}} \left[\mathrm{erf}\left\{\frac{\lambda_i}{\mathrm{i}\sqrt{2B}}\right\} - \mathrm{erf}\left\{\frac{\lambda_i(1+BT)}{\mathrm{i}\sqrt{2B}}\right\}\right]. \tag{27}$$

This expression is easily evaluated in symbolic algebra packages or even in advanced spreadsheets that include error functions and Bessel functions. For completeness, note that erf{i$z$} can alternatively be expressed as −i(erfi{$z$}), where erfi is the imaginary error function. The limiting case of $B = 0$ is analytically correct, but would involve division by zero if evaluated directly. However, this case corresponds to constant viscosity, which is considered above.

Figure 2 shows evolutions of the mean velocity and acceleration, obtained from Equation (27) using the inversion formulae in Equations (14) and (16). Also shown is the wall shear stress, which follows from Equation (18). Clearly, the viscosity cannot increase indefinitely so the graphs will be of no practical significance at very large times, but the trends at shorter times are revealing.

In Figure 2(a), the mean velocity is scaled by the mean velocity of a simple Poiseuille flow based on the prescribed pressure gradient and the initial viscosity. For the constant viscosity case ($B$=0), the velocity rises almost to its final steady state value in a non-dimensional time $T \approx 1$. For the increasing-viscosity cases, it initially rises in a similar manner, but subsequently departs from the constant-viscosity trend, reaches a maximum and decays towards zero as the viscosity tends to infinity. The greater the rate of increase of viscosity (i.e. large values of $B$), the smaller the velocity at any instant and the stronger the departure from the constant-viscosity trend.

In Figure 2(b), the acceleration is scaled by its initial value which, since the flow is initially stationary, is equal to the impressed pressure gradient, $P_0$. For the constant-viscosity case ($B$=0), the acceleration decreases continuously as the flow increases towards its new steady state. For the

increasing-viscosity cases ($B>0$), the acceleration is initially positive, but becomes negative after the velocity peaks. This behaviour is reflected in the history of the wall shear stress, which exceeds its asymptotic limit during the deceleration. In the Figure, the shear stress is scaled by $\rho a P_0/2$ – see Equation (18).

The periods of overshooting wall shear stress and negative acceleration are evidence that the velocity profiles during the flow development differ from quasi-steady (parabolic) profiles. This is confirmed in Figure 2(c), which shows evolving velocity profiles, obtained from Equation (27) using the inversion formula expressed in Equation (13) and scaled by the increasing instantaneous velocity at $r=0$. At sufficiently small times, the viscosity is nearly equal to $\nu_0$, irrespective of the value of $B$, and so the profiles, which are very flat, are almost indistinguishable from one another. As time increases, higher-viscosity cases (large $B$) approach the asymptotic condition more rapidly than lower-viscosity cases and so their profiles approach quasi-steady shapes more rapidly.

## LINEARLY INCREASING PRESSURE GRADIENT

Now consider the case of an imposed pressure gradient that increases in time. In the particular example presented, the prescribed increase is linear and the fluid is initially at rest. Neither of these choices is necessary, but they simplify both the analytical development and the interpretation of the resulting behaviour. Additionally, the chosen pressure gradient increases linearly *from zero*. This is another convenient simplification, but it does not really result in a loss of generality because the solution can be combined linearly with that for a step change in pressure gradient as follows.

In general, the prescribed linear variation of the pressure gradient function (Equation 2) is

$$P\{t\} = P_0 + P_1 t \tag{28}$$

where $P_0$ is the initial steady value and $P_1$ is the rate of increase with time. The case of ($P_0\neq 0, P_1=0$) is considered in the previous section and the case of ($P_0=0, P_1\neq 0$) is now considered. Equation (12) gives

$$\overline{u}\{g_i,t\} = \frac{aP_1 \mathrm{J}_1\{ag_i\}}{g_i}\exp\left[-(\nu_0 g_i^2)\int_0^t n\{\theta\}\mathrm{d}\theta\right] \left(\int_0^t \theta \exp\left[(\nu_0 g_i^2)\int_0^\theta n\{\psi\}\mathrm{d}\psi\right]\mathrm{d}\theta\right). \tag{29}$$

### Constant viscosity

When the viscosity is constant, $n\{t\}=1$. Using the non-dimensional time $T$ and the Bessel function zeros $\lambda_i=ag_i$, Equation (29) yields

$$\overline{u}\{\lambda_i,t\} = \frac{P_1 a^6 \mathrm{J}_1\{\lambda_i\}}{\nu_0^2 \lambda_i^3}\left[T-(1-\exp\{-\lambda_i^2 T\})/\lambda_i^2\right]. \tag{30}$$

The velocities, acceleration and shear stress follow from the appropriate inverse FHT and other formulae, all given in Equations (13)–(18). When $T=0$, the exponential term $\exp\{-\lambda_i^2 T\}$ is equal to unity and so the FHT of the velocity is zero (as prescribed). When $T$ is very small, the exponential is approximately equal to $1-\lambda^2 T+\lambda^4 T^2/2$ and so the transformed velocity increases with order $T^2$. When $T$ is large, the exponential tends to zero and the transformed velocity

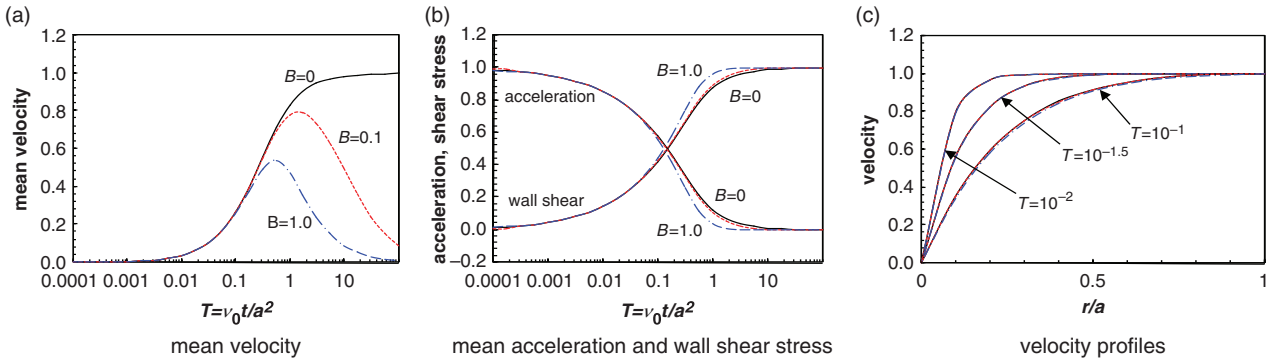


**Figure 3** | Starting flows resulting from a ramp pressure gradient [$B$=0 (continuous lines), $B$=0.1 (dotted lines), $B$=1.0 (dashed–dotted lines)]: (a) mean velocity, (b) mean acceleration and wall shear stress, and (c) velocity profiles.

increases with order $T$. The result for this simple case is identical to that obtained by Chambré *et al.* (1978).

Predicted evolutions of the mean velocity, mean acceleration and velocity profile are shown as the case labelled $B$=0 in Figure 3. They are discussed in the following section as limiting cases of behaviour with time-varying viscosity.

### Linearly increasing viscosity

By substituting Equation (25) into Equation (29), the FHT of the velocity for a linearly increasing viscosity and a linearly increasing pressure gradient is found to satisfy

$$\overline{u}\{g_i,t\} = \frac{P_1 a J_1\{ag_i\}}{v_0\beta_1 {g_i}^3\sqrt{2}}\left(1+\exp\{-v_0 {g_i}^2(2t+\beta_1 t^2)/2\}\right.$$
$$\left[-1+g_i\frac{\sqrt{\pi}}{\sqrt{-2\beta_1/v_0}}\left(\operatorname{erf}\left\{\frac{g_i(1+\beta_1 t)}{\sqrt{-2\beta_1/v_0}}\right\}\right.\right.$$
$$\left.\left.\left.-\operatorname{erf}\left\{\frac{g_i}{\sqrt{-2\beta_1/v_0}}\right\}\right)\right]\right) \qquad (31)$$

The corresponding behaviour of the mean velocity, etc, follow from the inverse FHT and other formulae in Equations (13)–(18) and are illustrated in Figure 3 for particular values of $B$ (and hence $\beta_1$) defined in Equation (26). The mean velocity is scaled by the mean velocity of a simple Poiseuille flow based on the increasing instantaneous value of the prescribed pressure gradient $P_1\{t\}$ and the initial viscosity $v_0$. With this scaling, the behaviour closely resembles that shown in Figure 2 for a step pressure gradient. Thus the asymptote attained for $B$=0 shows that the velocity is responding quasi-statically to the increasing pressure gradient. In the cases with increasing viscosity, the rate of flow initially increases, but it reaches a peak and then decays to zero because both the scaling velocity and the viscosity are increasing linearly. The greater the rate of increase of viscosity (larger $B$), the sooner the velocity peaks and decays to zero.

The acceleration of the mean flow is scaled using the instantaneous pressure gradient and is initially unity, but reduces rapidly and decays to zero. For the cases investigated, there is no overshoot equivalent to that found above for a suddenly imposed pressure gradient. As a consequence, there is also no overshoot in the wall shear stress, which is scaled by $\rho a P_1 t/2$ in Figure 3. The absence of these overshoots can be explained by regarding the ramp increase in pressure as a series of instantaneous step increases. The small-time consequences of the most recent steps dominate the large-time consequences of the less recent steps (compare the behaviours at small times and large times in Figure 2).

The velocity profiles (Figure 3(c)) show a smaller dependence on the rate of increase of viscosity than that obtained for the step change of pressure gradient (Figure 2(c)). The behaviour is qualitatively similar, but the on-going increase in the imposed pressure gradient tends to cause flatter profiles.

## OSCILLATING PRESSURE GRADIENT

The preceding examples represent types of flow that might occur quite commonly in practice, but they are also relatively simple. The following example describes a flow that will occur less commonly, but illustrates the generality of the analytical approach. It combines two features that are common in practice, namely a periodic variation of the forcing pressure gradient and a periodic variation of the viscosity. For generality, the assumed forcing frequencies are different although they would often be equal in practice. In both cases, the prescribed periodicity is sinusoidal, thereby leading once again to an analytical solution. Less simple forcing periodicity might necessitate a numerical solution or, perhaps, a series of analytical solutions for individual frequency components.

With an imposed periodic pressure gradient function of frequency $\omega_p$ and amplitude $P_A$ defined by

$$P\{t\} = P_A \sin\{\omega_p t\} \qquad (32)$$

the FHT of the velocity is found from Equation (12) as

$$\overline{u}\{g_i,t\} = \frac{aP_A J_1\{ag_i\}}{g_i}\exp\left\{-g_i^2 v_0\int_0^t n\{\theta\}\mathrm{d}\theta\right\}$$
$$\left(\int_0^t \sin\{\omega_p\theta\}\exp\left\{g_i^2 v_0\int_0^\theta n\{\psi\}\mathrm{d}\psi\right\}\mathrm{d}\theta\right). \qquad (33)$$

The viscosity variation is defined as

$$n\{t\} = 1+\beta_0+\beta_A\sin\{\omega_v t\} \qquad (34)$$

in which the pulsating viscosity frequency $\omega_v$ is taken to be different from the oscillating pressure frequency $\omega_p$. The

parameter $\beta_0$ is constant and, for physical reasons, the amplitude $\beta_A$ of the pulsation must not exceed $\beta_0$. Note that the parameters $\beta_0$ and $\beta_A$ are dimensionless. For this case, Equation (33) becomes

$$\overline{u}\{g_i,t\} = \frac{aP_A \mathrm{J}_1\{ag_i\}}{g_i}\int_0^t \sin\{\omega_p\theta\}\exp\{-g_i^2\nu_0([1+\beta_0](t-\theta) - (\beta_A/\omega_v)[\cos\{\omega_v t\} - \cos\{\omega_v\theta\}])\}\mathrm{d}\theta \quad (35)$$

and, once again, the corresponding behaviours of the mean velocity, etc, follow from the inverse FHT and other formulae in Equations (13)–(18).

## Constant viscosity

For the particular case of *constant*, i.e. Newtonian, viscosity ($\beta_0 = 0$, $\beta_A = 0$), Equation (33) leads to

$$\overline{u}\{t,\zeta_i\} = \frac{P_A a^2 \mathrm{J}_1\{\lambda_i\}[k_i\sin\{\omega_p t\} - \omega_p\cos\{\omega_p t\} + \omega_p\exp\{-k_i t\}]}{\lambda_i(k_i^2+\omega_p^2)} \quad (36)$$

where

$$k_i = \frac{\lambda_i^2\nu_0}{a^2}. \quad (37)$$

The inverse transform of Equation (36) is consistent with the expressions in Celnik *et al.* (2006) and is analogous to those obtained by Sexl (1930) or Uchida (1956) using a cosine forcing function. Once again, however, the above development is more straightforward. The predicted flow behaviour is discussed in the following section along with the corresponding behaviour for periodically varying viscosity.

## Pulsating viscosity

Figure 4(a) illustrates the variation of the mean velocity for a particular case with a pulsating viscosity frequency $\omega_v$ equal to $\frac{3}{4}$ of the pressure gradient frequency $\omega_p$. The velocity for a viscosity pulsation with $\beta_0$=1 and $\beta_A$=1 is compared with that for Newtonian viscosity (i.e. $\beta_0$=0, $\beta_A$=0). In all cases, the velocity is scaled with a quasi-steady value based on the maximum pressure gradient and the minimum viscosity (i.e. $\beta_0$). The forcing pressure gradient is also shown for comparison, using a reduced scale to avoid confusion with the velocity graphs.

Consider first the Newtonian case (i.e. viscosity function $n\{t\}$=1). This exhibits well-known behaviour, with the velocity varying in a simple harmonic manner, but lagging behind the forcing frequency. Qualitatively similar behaviour would be expected with the pulsating viscosity if its forcing frequency were equal to the pressure gradient frequency. In Figure 4(a), however, the use of different values for the two forcing frequencies $\omega_v$ and $\omega_p$ leads to beating. That is, greater amplitudes occur at some peaks and smaller amplitudes occur at others.

Figure 4(b) shows evolutions of the mean acceleration and the wall shear stress, scaled by the maximum pressure gradient $P_A$ and $\rho a P_A/2$, respectively. For clarity, results are shown for only one pulsating viscosity in addition to the Newtonian case. The qualitative behaviour follows predictably from that observed for the mean velocity. One result with potential practical implications, however, is that the deviation of the wall shear stress from the Newtonian case is much smaller than the corresponding deviation of the mean velocity.

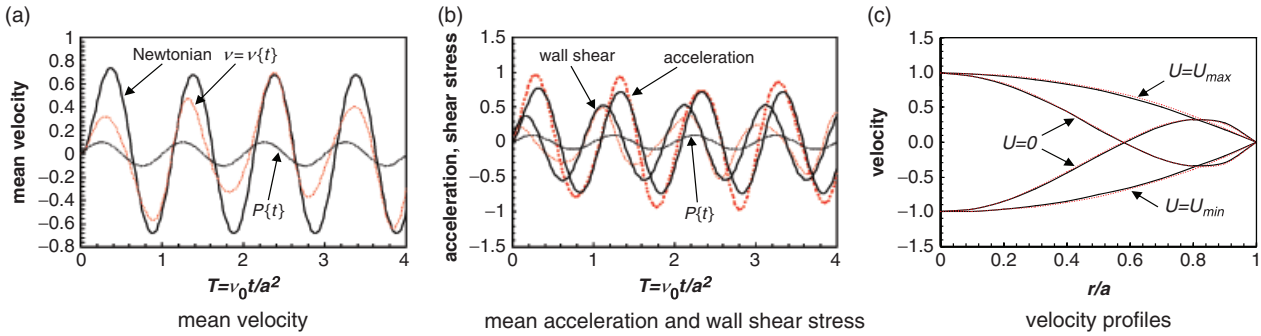


**Figure 4** | Periodic flows resulting from an oscillating pressure gradient [Newtonian (continuous lines), *n=n{t}* (dotted lines)]: (a) mean velocity, (b) mean acceleration and wall shear stress, and (c) velocity profiles.

Figure 4(c) shows velocity profiles at various instants. In each case, the velocity is scaled by the instantaneous centreline velocity, which itself varies strongly. This highlights large differences from quasi-steady profiles that occur during periods of flow reversal. For example, velocity gradients exist at the wall at the instants when the mean velocity is zero. Indeed, different velocity profiles are obtained at $U = 0$ according to whether the flow is accelerating or decelerating. This behaviour, which occurs even for the case of constant viscosity, is consistent with the out-of-phase relationships seen in Figure 4(a, b) between the mean velocity, mean acceleration, shear stress and the forcing pressure gradient.

## CONCLUSIONS

A *general* solution has been obtained for unsteady pipe flows with any prescribed temporal variations of imposed pressure gradient and fluid viscosity. For some prescribed variations of these parameters, the resulting flows can be described in analytical form. For all others, the need for numerical solution is restricted to the equivalent of evaluating areas under piece-wise smooth curves.

The general solution is developed using finite Hankel transforms (FHT) and the prescribed time-varying pressure gradient and viscosity are substituted into a general expression for the transformed velocity. This does not result in any loss of generality because the physical parameters (velocity, acceleration, shear stress, etc) follow directly using particular forms of the standard inverse finite Hankel transform (IFHT).

To illustrate the use of the general solution, examples have been presented for three types of varying pressure gradient, namely a sudden step increase, a linear increase and a sinusoidal fluctuation. In each case, solutions for prescribed varying viscosity have been compared with those for constant viscosity (i.e. a Newtonian fluid).

For the special case of a constant viscosity, solutions are already available in the literature for each of the cases presented herein. Of necessity, the present solution using FHT is exactly equivalent to the previously published solutions. Nevertheless, the FHT method of obtaining the solution is considerably simpler than the previously published methods.

The particular examples used to illustrate the use of the method for varying viscosity are directly applicable to unsteady flows with viscosity based on prescribed temperature dependence. An important future application of the method will be its use in increasing understanding of time-dependent turbulent viscosity typical of that observed in accelerating and decelerating pipe flows.

## REFERENCES


Abramowitz, M. & Stegun, I. A. 1972 *Handbook of Mathematical Functions*. Dover, New York, p 484.

Achard, J. L. & Lespinard, G. M. 1981 Structure of the transient wall-friction law in one-dimensional models of laminar pipe flows. *J. Fluid Mech.* **113**, 283–298.

Adegbie, K. S. & Alao, F. I. 2006 Flow of a Newtonian fluid in a symmetrically heated channel: effect of viscosity and viscous dissipation. *Math. Problems Engng.* **2006**, 1–7.

Barnes, H. A. 1997 Thixotropy–a review. *J. Non-Newtonian Fluid Mech.* **70**, 1–33.

Boyce, W. E. & DiPrima, R. C. 1969 *Elementary Differential Equations and Boundary Value Problems* 2nd edn. Wiley, New York, p 14.

Butler, F. & O'Donnell, H. J. 1999 Modelling the flow of a time-dependent viscous product (cultured buttermilk) in a tube viscometer at 5°C. *J. Food Engng.* **42**, 199–206.

Celnik, M. S., Patel, M. J., Pore, M., Scott, D. M. & Wilson, D. I. 2006 Modelling laminar pulsed flow for the enhancement of cleaning. *Chem. Engng. Sci.* **61**, 2079–2084.

Chambré, P. L., Schrock, V. E. & Gopalakrishnan, A. 1978 Reversal of laminar flow in a circular pipe. *Nucl. Engng. Design* **47**, 239–250.

Costa, A. & Macedonio, G. 2003 Viscous heating in fluids with temperature-dependent viscosity: implications for magma flows. *Non-Linear Process. Geophys.* **10**, 545–555.

Costa, A., Melnik, O. & Vedeneeva, E. 2007 Thermal effects during magma ascent in conduits. *J. Geophys. Res.* **112**, B12205, (doi: 10.1029/2007JB004985).

Debnath, L. & Bhatta, D. 2007 *Integral Transforms and Their Applications* 2nd edn. Chapman & Hall/CRC, Boca Raton, FL.

Erdogan, M. E. & Imrak, C. E. 2007a On the comparison of the methods used for the solutions of the governing equation for unsteady unidirectional flows of second grade fluids. *Int. J. Engng. Sci.* **45**, 786–796.

Erdogan, M. E. & Imrak, C. E. 2007b On some unsteady flows of a non-Newtonian fluid. *Appl. Math. Modell.* **31**, 170–186.

Erdogan, M. E. & Imrak, C. E. 2009 On the comparison of the solutions obtained using two different transform methods for the second problem of Stokes for Newtonian fluids. *Int. J. Non-Linear Mech.* **44**, 27–30.

Fetecau, C. 2004 Analytical solutions for non-Newtonian fluid flows in pipe-like domains. *Int. J. Non-Linear Mech.* **39**, 225–231.

Fetecau, C. & Fetecau, C. 2005 Starting solutions for some unsteady unidirectional flows of a second grade fluid. *Int. J. Engng. Sci.* **43**, 781–789.

Hayat, T., Khan, M. & Ayub, M. 2006 Some analytical solutions for second grade fluid flows for cylindrical geometries. *Math. Comput. Modell.* **43**, 16–29.

He, S., Ariyaratne, C. & Vardy, A. E. 2008 A computational study of wall friction and turbulence dynamics in accelerating pipe flows. *Comput. Fluids* **37**(6), 674–689.

Maingonnat, J. F., Muller, L. & Leuliet, J. C. 2005 Modelling the build-up of a thixotropic fluid under viscosimetric and mixing conditions. *J. Food Engng.* **71**, 265–272.

Massoudi, M. & Phuoc, T. X. 2006 Unsteady shear flow of fluids with pressure-dependent viscosity. *Int. J. Engng. Sci.* **44**, 915–926.

Ng, C -O. 2004 A time-varying diffusivity model for shear dispersion in oscillatory channel flow. *Fluid Dyn. Res.* **34**, 335–355.

Phan-Thien, N. 2002 *Understanding Viscoelasticity*. Springer, Berlin.

Schowalter, W. R. 1977 *Mechanics of Non-Newtonian Fluids*. Pergamon, Oxford.

Sexl, T. 1930 Über den von E.G.Richardson entdeckten "Annulareffekt". *Z. Phys.* **61**, 349–362.

Sneddon, I. N. 1951 *Fourier Transforms*. McGraw-Hill, New York.

Sneddon, I. N. 1972 *The Use of Integral Transforms*. McGraw-Hill, New York.

Suslova, S. A. & Tran, T. D. 2008 Revisiting plane Couette–Poiseuille flows of a piezo-viscous fluid. *J. Non-Newtonian Fluid Mech.* **154**, 170–178.

Szymanski, P. 1932 Quelques solutions exactes des equations de l'hydrodynamique et du fluide visqueux dans le cas d'un tube cylindrique. *J. Math. Pures Appl.* **11**, 67–107.

Uchida, S. 1956 The pulsating viscous flow superposed on the steady laminar motion of incompressible fluid in a circular pipe. *Z. Angew. Math. Phys.* **7**, 402–422.

Vasudevaiah, M. & Rajagopal, K. R. 2005 On fully developed flows of fluids with a pressure dependent viscosity in a pipe. *Appl. Math.* **50**, 341–353.

First received 14 September 2009; accepted in revised form 7 April 2010. Available online 1 October 2010